STUDY ON CONTACT PATCH MEMORY AND TRAVELLING WAVES OF TYRES

Dénes Takács[1], Gábor Stépán[2]
[1]MTA-BME Research Group on Dynamics of Machines and Vehicles
[2]Department of Applied Mechanics, Budapest University of Technology and Economics
Műegyetem rkp. 3.
H-1111 Budapest, Hungary
e-mail address of lead author: takacs@mm.bme.hu

In this study, the self-excited vibrations of the caster-wheel system are analysed. A low degree-of-freedom mechanical model is considered, in which the lateral deformation of the tyre is described both in the contact patch and outside it. The simple brush tyre model is implemented in order to obtain analytical results by means of minimum number of relevant parameters. The frequencies of the detected self-excited vibrations are presented against the towing speed. Some intricate shapes of the corresponding tyre deformations are presented based on numerical simulations.

1 INTRODUCTION

The shimmy of towed wheels (e.g. the front wheels of motorcycles [1, 2], the nose-gears of air-planes [3, 4, 5]) is a fascinating phenomenon in vehicle dynamics. The safety hazard of shimmy induced many publications in the field, but the elimination of shimmy requires special attention from engineers even nowadays. On the one hand, towed wheels are often parts of complex vehicle systems, which require the analyses of multi-body systems like the fuselage of air-planes [4]. On the other hand, the investigation of shimmy demands improved and detailed models of tyres and tyre/road interactions.

The memory effect of the tyre/ground contact patch was already recognized in [6]. However, the available mathematical methods did not provide opportunity for engineers at that time to analyse delay differential equations. An engineering approximation of the tyre lateral deformation in the contact patch helped to describe some behaviour of the caster-wheel system [7, 8]. Later, the accurate modelling of the contact patch lateral deformation and the analysis of the corresponding delay differential equations provided new explanations for some quasi-periodic vibrations [9].

The noise generation of tyres has become an important research field in tyre dynamics, which makes the developments of different theoretical models of tyre/road interaction to be a relevant topic again (see, for example, [10, 11, 12, 13]). The mechanical models usually consider the radial and/or the longitudinal deformation of the tyre thread elements. However, the lateral vibration of vehicles can also lead to such periodic tyre deformations that can generate noise and wear (see [14]). The application of the time delayed tyre model in the single track car model [15] also identified parameter domains where small amplitude lateral vibrations may appear leading to enhanced noise and heat generation.

In this study, a simple mechanical model of a shimmying wheel is constructed, in which the lateral deformations are described both inside and outside the contact patch. The delayed contact patch model is combined with a simple tyre carcass model. Critical parameter ranges of self-excited vibrations are determined versus the longitudinal speed of the towed tyre with special attention to the vibration frequencies. Tyre deformations are illustrated by means of numerical simulations at certain towing speeds.

2 MECHANICAL MODEL

The mechanical model is shown in Figure 1. The wheel of elastic tyre is attached to the rigid caster of length l. The caster is pulled at the king pin A with the constant towing speed v, R refers to the outer radius of the tyre, and it contacts to the ground at a contact patch of length $2a$. One of the state variables is the caster angle denoted by $\psi(t)$. The lateral deformations of the tyre are described with the help of the lateral deformation $q(x,t)$ of the centre line of the contact patch. This will serve as another state variable that is a distributed one along the coordinate x attached to the caster. For the sake of simplicity,

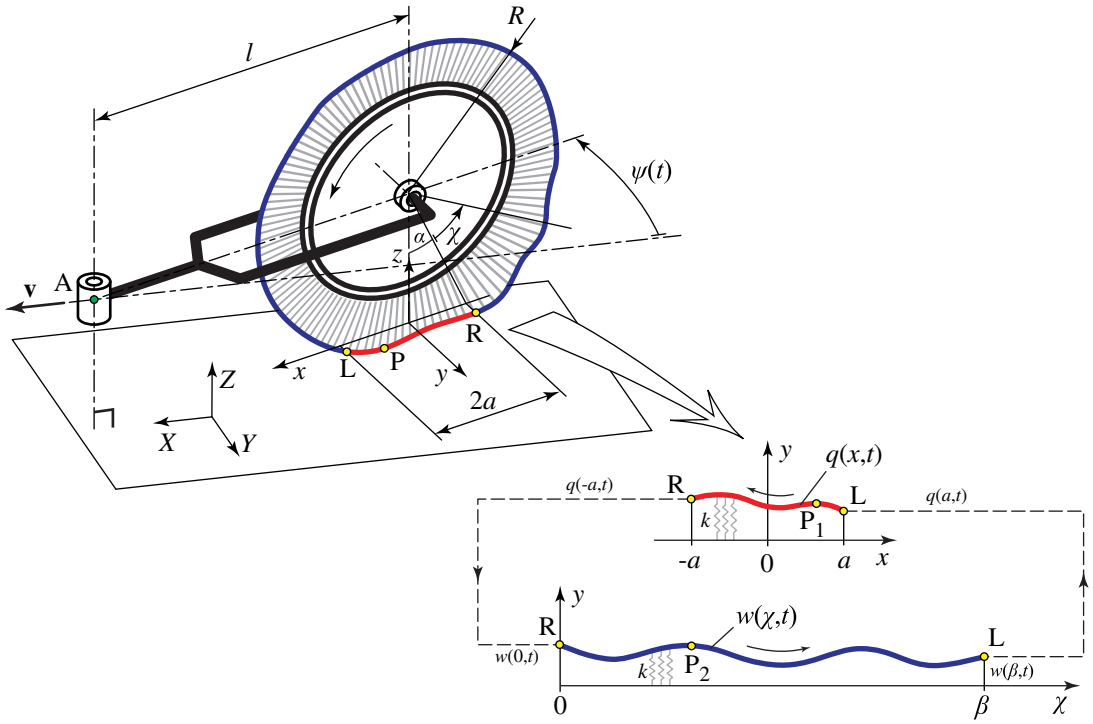

Figure 1: The mechanical model

pure rolling of the tyre is considered. Outside the contact patch, along the circumference of the tyre, the vibrations of the thread elements are described by the lateral deformation function $w(\chi, t)$, which is an extended distributed state variable. The angle $\chi \in [0, \beta]$ (where $\beta = 2(\pi - \alpha)$ and $\alpha = \arcsin(a/R)$) sweeps along the circumference of the tyre starting from the trailing edge R and ending at the leading edge L of the contact patch.

In this study, we use the so-called brush tyre model, which considers separated tyre particles along the circumference of the tyre. Here, the threads are modelled by means of continuously distributed masses supported by springs. These inertial and elastic properties are characterized by $\rho A\,[\mathrm{kg/m}]$ and $k\,[\mathrm{N/m^2}]$, respectively.

2.1 Lateral deformation in the contact patch

Due to the fact that we consider pure rolling, the tyre particles attached to the ground have zero velocities. The position vector of a tyre particle P_1 can be written in the (X, Y, Z) ground-fixed coordinate system as

$$\mathbf{R}_{\mathrm{P}_1} = \begin{bmatrix} vt - (l-x)\cos\psi(t) - q(x,t)\sin\psi(t) \\ -(l-x)\sin\psi(t) + q(x,t)\cos\psi(t) \\ 0 \end{bmatrix}, \tag{1}$$

for $x \in [-a, a]$. The kinematic constraint of rolling means that $\frac{\mathrm{d}}{\mathrm{d}t}\mathbf{R}_{\mathrm{P}_1} = \mathbf{0}$, which leads to partial differential equation (PDE) characterizing the lateral deformations in the contact patch (see details [16]). Here we present its linearised form only:

$$\dot{q}(x,t) = v\psi(t) + (l-x)\dot{\psi}(t) + q'(x,t)v\,, \tag{2}$$

for $x \in [-a, a]$. In our study, dot and prime refer to the partial derivatives with respect to time t and the space coordinates, respectively.

2.2 Lateral deformation outside the contact patch

The equations of motion of the tyre particles outside the contact patch are determined with Hamilton's Principle. The Lagrangian can be written as the difference of the kinetic energy and the potential function

of the spring forces:

$$L = \frac{1}{2}\int_0^\beta \left(\rho A \mathbf{v}_{\mathrm{P}_2}^2(\chi,t) - k w^2(\chi,t)\right) R\mathrm{d}\chi\,, \tag{3}$$

where $\mathbf{v}_{\mathrm{P}_2}(\chi,t)$ refers to the velocity of the tyre particle at the position χ:

$$\mathbf{v}_{\mathrm{P}_2}(\chi,t) = \begin{bmatrix} v\cos\psi(t) - w(\chi,t)\dot{\psi}(t) - v\cos(\alpha+\chi) \\ -v\sin\psi(t) - (l + R\sin(\alpha+\chi))\dot{\psi}(t) + \dot{w}(\chi,t) + \frac{v}{R}w'(\chi,t) \\ v\sin(\alpha+\chi) \end{bmatrix}. \tag{4}$$

Here we assumed that the translational rate of change of the tyre particles are equal to the towing speed v. This approximation is acceptable in case of small amplitude vibrations of the towed wheel.

According to Hamilton's Principle, the action functional $I = \int L\,\mathrm{d}t$ is extremal for the realized motion of the system, i.e. $\delta I = 0$. This weak form of the equation of motion can be transformed into the form of differential equations by means of the Euler–Lagrange equation. Considering (4) in (3), the action reads

$$I = \int_{t_0}^{t_1}\int_0^\beta F(w,\dot{w},w',\chi,t)\,\mathrm{d}\chi\mathrm{d}t\,, \tag{5}$$

and the Euler-Lagrange equation leads to

$$\frac{\mathrm{d}F}{\mathrm{d}w} - \frac{\partial}{\partial t}\frac{\partial F}{\partial \dot{w}} - \frac{\partial}{\partial \chi}\frac{\partial F}{\partial w'} = 0\,. \tag{6}$$

Considering small amplitude vibrations, the tyre deformation is characterized by the linearised partial differential equation:

$$\ddot{w}(\chi,t) + \frac{2v}{R}\dot{w}'(\chi,t) + \frac{v^2}{R^2}w''(\chi,t) + \omega_{\mathrm{c}}^2 w(\chi,t) = (l + R\sin(\alpha+\chi))\,\ddot{\psi}(t) + 2v\,\dot{\psi}(t)\cos(\alpha+\chi), \tag{7}$$

for $\chi \in [0,\beta]$. The natural angular frequency $\omega_{\mathrm{c}} = \sqrt{k/\rho A}$ represents the free lateral vibrations of the tyre brush elements.

2.3 Equation of motion of the caster-wheel system

The equation of motion of the caster-wheel rigid-body system can be derived with the help of Newton's Law:

$$J_{\mathrm{A}}\ddot{\psi}(t) = -k\int_{-a}^{a}(l-x)q(x,t)\,\mathrm{d}x - k\int_0^\beta (l + R\cos(\alpha+\chi))w(\chi,t)\,R\mathrm{d}\chi\,, \tag{8}$$

where J_{A} is the mass moment of inertia of the caster-wheel system with respect to the z axis at the king pin A.

The equation of motion (8) is coupled to (2) and (7). The boundary conditions (BCs) of the PDEs are:

$$\begin{aligned} q(a,t) &= w(\beta,t)\,, \\ w(0,t) &= q(-a,t)\,, \\ w'(0,t) &= -Rq'(-a,t)\,. \end{aligned} \tag{9}$$

The first two BCs ensure the continuity of the lateral deformation at the leading edge L and at the trailing edge R, respectively. The third one (no kink at R) refers to $\frac{\mathrm{d}}{\mathrm{d}t}w(0,t) = \frac{\mathrm{d}}{\mathrm{d}t}q(-a,t)$, which describes the initial lateral speed of the deformation waves that propagate along the circumference of the tyre outside the contact patch.

3 TIME DELAYED TYRE MODEL

3.1 Travelling wave in the contact patch

The memory effect of the tyre/ground contact patch is known since von Schlippe already identified this property of tyres in [6]. In case of rolling, the tyre particles stick to the ground and keep their positions during the contact. Consequently, their positions at the time instant t were determined when they reached the ground at the leading edge at the earlier time instant $t-\tau_1(x)$. The time delay $\tau_1(x)$ characterizes the time needed for a tyre particle to travel backwards in the contact patch from the leading edge L to its actual position x (see Figure 1). Thus, the travelling wave solution of the PDE (2) can be determined in the form:

$$q(x,t) = (l-a+v\tau_1(x))\psi(t) - (l-a)\psi(t-\tau_1(x)) + q(a,t-\tau_1(x)) \tag{10}$$

for $x \in [-a,a]$. In this linear approximation, the time delay has a physically obvious form:

$$\tau_1(x) = \frac{a-x}{v}\,. \tag{11}$$

3.2 Travelling wave solution outside the contact patch

Since the translational speed of tyre particles along the circumference of tyre is approximately constant when the vibrations are small, a traveling wave solution can also be composed for (7). The application of Duhamel's integral formula leads to

$$\begin{aligned} w(\chi,t) = {} & w(0,t-\tau_2(\chi))\cos(\omega_\mathrm{c}\tau_2(\chi)) \\ & + \frac{1}{\omega_\mathrm{c}}\frac{\mathrm{d}}{\mathrm{d}t}w(0,t-\tau_2(\chi))\sin(\omega_\mathrm{c}\tau_2(\chi)) \\ & + \frac{1}{\omega_\mathrm{c}}\int_0^{\tau_2(\chi)}\left(l+R\sin\left(\alpha+\frac{v}{R}\vartheta\right)\right)\ddot{\psi}(t-\tau_2(\chi)+\vartheta)\sin(\omega_\mathrm{c}(\tau_2(\chi)-\vartheta))\mathrm{d}\vartheta \\ & + \frac{1}{\omega_\mathrm{c}}\int_0^{\tau_2(\chi)}2v\,\dot{\psi}(t-\tau_2(\chi)+\vartheta)\cos\left(\alpha+\frac{v}{R}\vartheta\right)\sin(\omega_\mathrm{c}(\tau_2(\chi)-\vartheta))\mathrm{d}\vartheta\,, \end{aligned} \tag{12}$$

where the time delay is

$$\tau_2(\chi) = \frac{R\chi}{v}\,. \tag{13}$$

3.3 Overall description of the lateral deformations

Using the second and the third BCs of (9), the travelling wave solution (12) can be composed as a function of the trailing edge deformation of the contact patch:

$$\begin{aligned} w(\chi,t) = {} & q(-a,t-\tau_2(\chi))\cos(\omega_\mathrm{c}\tau_2(\chi)) \\ & + \frac{1}{\omega_\mathrm{c}}\frac{\mathrm{d}}{\mathrm{d}t}q(-a,t-\tau_2(\chi))\sin(\omega_\mathrm{c}\tau_2(\chi)) \\ & + \frac{1}{\omega_\mathrm{c}}\int_0^{\tau_2(\chi)}\left(l+R\sin\left(\alpha+\frac{v}{R}\vartheta\right)\right)\ddot{\psi}(t-\tau_2(\chi)+\vartheta)\sin(\omega_\mathrm{c}(\tau_2(\chi)-\vartheta))\mathrm{d}\vartheta \\ & + \frac{1}{\omega_\mathrm{c}}\int_0^{\tau_2(\chi)}2v\,\dot{\psi}(t-\tau_2(\chi)+\vartheta)\cos\left(\alpha+\frac{v}{R}\vartheta\right)\sin(\omega_\mathrm{c}(\tau_2(\chi)-\vartheta))\mathrm{d}\vartheta\,. \end{aligned} \tag{14}$$

Using the travelling wave solution (10), the trailing edge deformation can be described:

$$\begin{aligned} q(-a,t-\tau_2(\chi)) = {} & (l+a)\psi(t-\tau_2(\chi)) - (l-a)\psi(t-\tau_2(\chi)-T_1) \\ & + q(a,t-\tau_2(\chi)-T_1)\,, \end{aligned} \tag{15}$$

where

$$T_1 = \tau_1(-a) \equiv \frac{2a}{v} \tag{16}$$

is the time interval that is needed for a tyre particle to travel in the contact patch from the leading edge L to the trailing edge R. The material time derivative at the leading edge can be calculated via (2):

$$\frac{\mathrm{d}}{\mathrm{d}t}q(-a,t-\tau_2(\chi)) = v\psi(t-\tau_2(\chi)) + (l+a)\dot{\psi}(t-\tau_2(\chi)) \tag{17}$$

After the substitution of (15) and (17) into (14), the first BC of (9) leads to

$$\begin{aligned} q(a,t) = {} & ((l+a)\psi(t-T_2) - (l-a)\psi(t-T_1-T_2))\cos(\omega_\mathrm{c}T_2) \\ & + q(a,t-T_1-T_2)\cos(\omega_\mathrm{c}T_2) + \frac{1}{\omega_\mathrm{c}}\left(v\psi(t-T_2) + (l+a)\dot{\psi}(t-T_2)\right)\sin(\omega_\mathrm{c}T_2) \\ & + \frac{1}{\omega_\mathrm{c}}\int_0^{T_2}\left(l + R\sin\left(\alpha+\frac{v}{R}\vartheta\right)\right)\ddot{\psi}(t-T_2+\vartheta)\sin(\omega_\mathrm{c}(T_2-\vartheta))\mathrm{d}\vartheta \\ & + \frac{1}{\omega_\mathrm{c}}\int_0^{T_2} 2v\,\dot{\psi}(t-T_2+\vartheta)\cos\left(\alpha+\frac{v}{R}\vartheta\right)\sin(\omega_\mathrm{c}(T_2-\vartheta))\mathrm{d}\vartheta\,, \end{aligned} \tag{18}$$

where

$$T_2 = \tau_2(\beta) \equiv \frac{R\beta}{v} \equiv \frac{2R(\pi-\alpha)}{v} \tag{19}$$

refers to the time needed for a tyre particle to travel along the circumference of the tyre from the trailing edge R to the leading edge L.

Using (10) and (14) with (15) in (8), one can eliminate the deformation functions $q(x,t)$ and $w(\chi,t)$. As a consequence, the corresponding PDEs (2) and (7) can be omitted, and the governing equations of the system reduce to:

$$\begin{aligned} & J_\mathrm{A}\ddot{\psi}(t) + 2ak\left(l^2+\frac{a^2}{3}\right)\psi(t) = kv\int_0^{T_1}(l-a+v\tau_1)\left((l-a)\psi(t-\tau_1) - q(a,t-\tau_1)\right)\mathrm{d}\tau_1 \\ & - kv\int_0^{T_2}\left(l+R\cos\left(\alpha+\frac{v}{R}\tau_2\right)\right)((l+a)\psi(t-\tau_2) - (l-a)\psi(t-T_1-\tau_2))\cos(\omega_\mathrm{c}\tau_2)\,\mathrm{d}\tau_2 \\ & - kv\int_0^{T_2}\left(l+R\cos\left(\alpha+\frac{v}{R}\tau_2\right)\right)q(a,t-T_1-\tau_2)\cos(\omega_\mathrm{c}\tau_2)\,\mathrm{d}\tau_2 \\ & - \frac{kv}{\omega_\mathrm{c}}\int_0^{T_2}\left(l+R\cos\left(\alpha+\frac{v}{R}\tau_2\right)\right)\left(v\psi(t-\tau_2)+(l+a)\dot{\psi}(t-\tau_2)\right)\sin(\omega_\mathrm{c}\tau_2)\,\mathrm{d}\tau_2 \\ & - \frac{kv}{\omega_\mathrm{c}}\int_0^{T_2}\left(l+R\cos\left(\alpha+\frac{v}{R}\tau_2\right)\right)\int_0^{\tau_2}\left(l+R\sin\left(\alpha+\frac{v}{R}\vartheta\right)\right)\ddot{\psi}(t-\tau_2+\vartheta)\sin(\omega_\mathrm{c}(\tau_2-\vartheta))\mathrm{d}\vartheta\,\mathrm{d}\tau_2 \\ & - \frac{kv}{\omega_\mathrm{c}}\int_0^{T_2}\left(l+R\cos\left(\alpha+\frac{v}{R}\tau_2\right)\right)\int_0^{\tau_2} 2v\,\dot{\psi}(t-\tau_2+\vartheta)\cos\left(\alpha+\frac{v}{R}\vartheta\right)\sin(\omega_\mathrm{c}(\tau_2-\vartheta))\mathrm{d}\vartheta\,\mathrm{d}\tau_2\,, \end{aligned} \tag{20}$$

which is coupled to (18). It can be seen that the substitution of the leading edge lateral deformation $q(a,t)$ leads to a neutral type distributed delay differential equation.

4 STABILITY ANALYSIS

One can substitute the exponential trial solutions $\psi(t) = P\mathrm{e}^{\lambda t}$ and $q(a,t) = Q\mathrm{e}^{\lambda t}$ into the linear governing equations (18) and (20) and can calculate the characteristic function $D(\lambda)$ of the system. Due to its complexity, we do not present the formula of the characteristic function here.

Self-excited vibrations of the caster-wheel system can be identified where the rectilinear motion becomes unstable. According to the D-subdivision method, the stability boundaries can be determined if we substitute $\lambda = \mathrm{i}\omega$ into the characteristic function with the real positive angular frequency ω and we separate its real and imaginary parts to be zeros. Unfortunately, the boundaries cannot be calculated in closed form but by means of numerical methods, one can construct stability charts. For example, using the multi-dimensional bisection method [17], stability boundaries can be determined in the multi-dimensional parameter space of the model.

Figure 2 shows some of these boundaries in the $v-l$ plane for the parameters $a = 0.04\,\mathrm{m}$, $R = 0.2\,\mathrm{m}$, $k = 60\,\mathrm{kN/m^2}$, $\rho A = 0.4\,\mathrm{kg/m}$ and $J_\mathrm{A} = 0.16\,\mathrm{kg/m^2}$, which are based on the laboratory

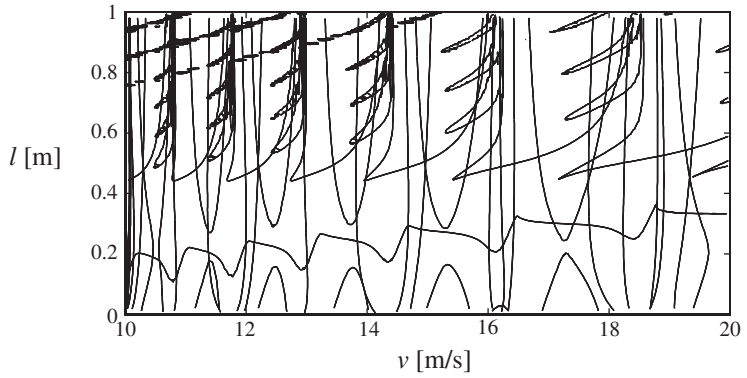

Figure 2: Stability boundaries in the $v - l$ parameter plane

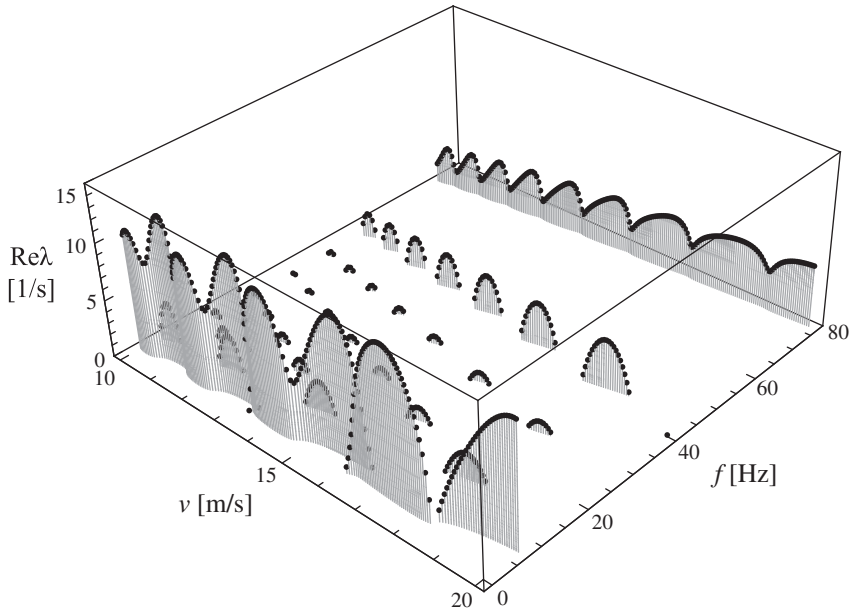

Figure 3: The variation of the characteristic roots versus the towing speed

experiments in [14]. The boundaries characterize the domains, where different kinds of self-excited vibrations occur with different frequencies. As it can be observed, lot of boundaries appear in the investigated parameter domain.

Let us consider the caster length $l = 0.5\,\mathrm{m}$, and let us show some properties of the emerging self-excited vibrations against the longitudinal speed v. The characteristic roots having positive real parts are shown in Figure 3 for the speed range $10 \ldots 20\,\mathrm{m/s}$. As it can be observed, the self-excited vibrations emerge in the whole speed range. The different projections of this chart are plotted in Figure 4. Both very low (1 Hz) and higher (80 Hz) vibration frequencies can be identified in the figure. Of course, our model does not consider the damping, which can strongly influence these result. The full stability analysis in the presence of damping will be the task of future research.

5 TYRE DEFORMATIONS

To check the theoretical results and to obtain information about the tyre deformations, numerical simulation was carried out. The original IDE-PDEs system (8), (2) and (7) were discretized by means of simple finite difference method. The number of spatial mesh points in the contact patch was chosen to 20 while outside the contact patch it was 300. The initial conditions for the numerical simulations were set to zero initial caster angle and zero lateral deformations, but non-zero initial angular speed of the

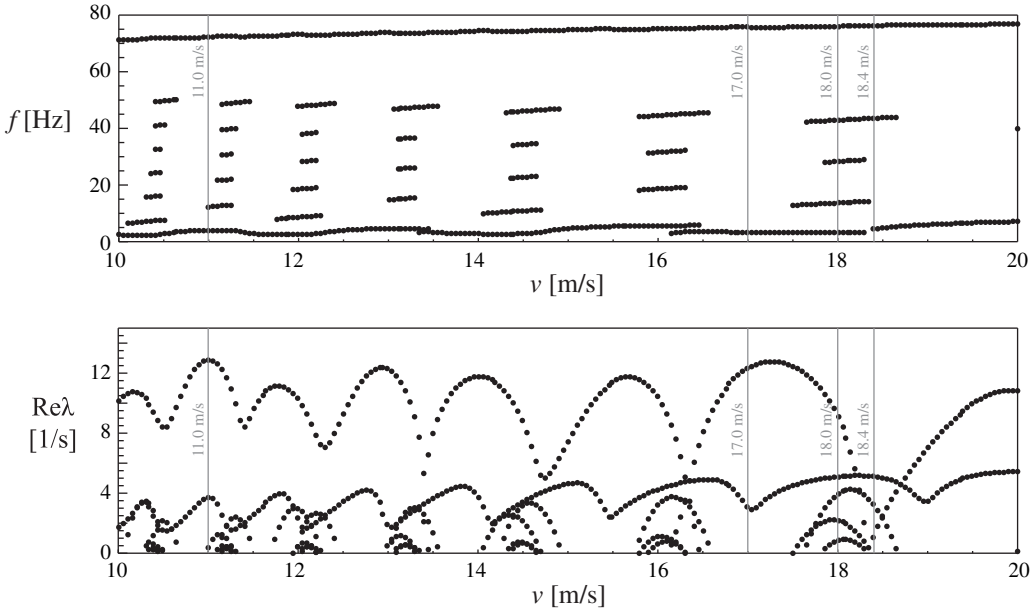

Figure 4: The real parts of the characteristic roots and corresponding vibration frequencies against the towing speed

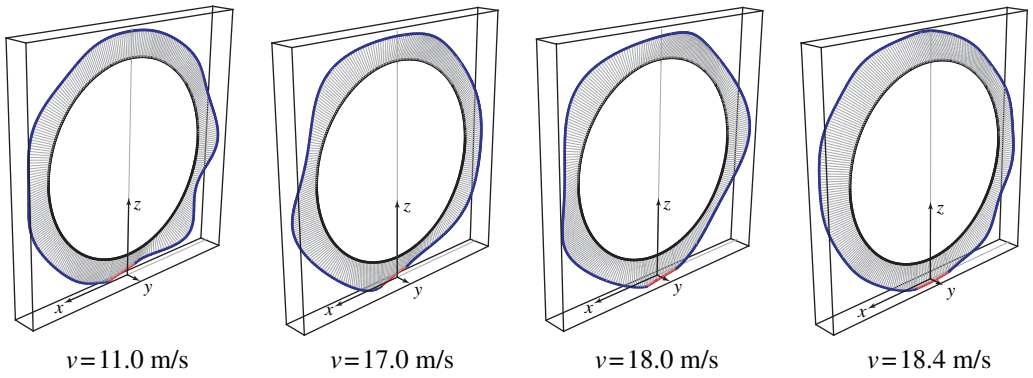

Figure 5: Tyre lateral deformation at different towing speeds

caster was considered.

Figure 5 shows the representative tyre deformation at different towing speeds, which speeds are also marked in Figure 4. Obviously, as the wheel speed increases the number of the waves decreases outside the contact patch, compare the deformations at the speeds 11.0 and 17.0 m/s. It is also worth to observe that small variation in the towing speed can strongly influence the vibration frequencies and the corresponding tyre deformations, see the cases that relate to the towing speeds 18.0 and 18.4 m/s.

6 CONCLUSION

A mechanical model was constructed to investigate the self-excited vibration of towed tyres. The delayed tyre/ground contact model was implemented. Moreover, the lateral tyre deformation was also considered outside the contact patch by means of the so-called brush model that also takes into account the mass of the tyre particles.

The governing equations of the system were determined as an IDE-PDE system and were transformed into the form of delay differential equations of the neutral type. It was shown that the interaction of the contact patch and the non-contacting tyre particles lead to tyre vibrations with various frequencies in a wide towing speed range. Although, damping was not considered in our study, some of the detected

vibrations can be the origin of noise and heat generation in practice even in the presence of damping.

Acknowledgement This research was partly supported by the János Bolyai Research Scholarship of the Hungarian Academy of Sciences and by the Hungarian National Science Foundation under grant no. OTKA PD105442.

REFERENCES

[1] V. Cossalter *Motorcycle Dynamics*, Lulu Editor, 2006.
[2] R.S. Sharp, S. Evangelou, and D.J.N. Limebeer, *Advances in the Modelling of Motorcycle Dynamics*, Multibody System Dynamics 12 (2004), pp. 251–283.
[3] I.J.M. Besselink, *Shimmy of Aircraft Main Landing Gears*, Technical University of Delft, The Netherlands, 2000.
[4] N. Terkovics, S. Neild, M. Lowenberg, and B. Krauskpof, *Bifurcation Analysis of a Coupled Nose Landing Gear-Fuselage System*, in *Proceedings of AIAA 2012* paper No. AIAA 2012-4731, Minneapolis, Minnesote, USA, 2012, pp. 1–14.
[5] C. Howcroft, B. Krauskopf, M. Lowenberg, and S. Neild, *Effects of Freeplay on Aircraft Main Landing Gear Stability*, in *Proceedings of AIAA 2012* paper No. AIAA 2012-4730, Minneapolis, Minnesote, USA, 2012, pp. 1–16.
[6] B. Schlippe and R. Dietrich, *Das Flattern Eines Bepneuten Rades (Shimmying of a pneumatic wheel)*, in *Bericht* 140 *der Lilienthal-Gesellschaft für Luftfahrtforschung* English translation is available in *NACA Technical Memorandum* 1365, pages 125-166, 217-228, 1954, 1941, pp. 35–45, 63–66.
[7] L. Segel, *Force and moment response of pneumatic tires to lateral motion inputs*, Journal of Engineering for Industry, Transactions of the ASME 88B (1966), pp. 37–44.
[8] H.B. Pacejka, *The Wheel Shimmy Phenomenon*, Technical University of Delft, The Netherlands, 1966.
[9] G. Stépán, *Delay, nonlinear oscillations and shimmying wheels*, in *Proceedings of Symposium CHAOS'97* Kluwer Ac. Publ., Dordrecht, Ithaca, N.Y., 1998, pp. 373–386.
[10] J. Cesbron, F. Anfosso-Lédée, D. Duhamel, H.P. Yin, and D.L. Houédec, *Experimental study of tyre/road contact forces in rolling conditions for noise prediction*, Journal of Sound and Vibration 320 (2009), pp. 125 – 144.
[11] P.B.U. Andersson and W. Kropp, *Rapid tyre/road separation: An experimental study of adherence forces and noise generation*, Wear 266 (2009), pp. 129–138.
[12] D. O'Boy and A. Dowling, *Tyre/road interaction noise – Numerical noise prediction of a patterned tyre on a rough road surface*, Journal of Sound and Vibration 323 (2009), pp. 270 – 291.
[13] R.J. Pinnington, *Tyre-road contact using a particle-envelope surface model*, Journal of Sound and Vibration 332 (2013), pp. 7055 – 7075.
[14] D. Takács and G. Stépán, *Micro-shimmy of towed structures in experimentally uncharted unstable parameter domain*, Vehicle System Dynamics 50 (2012), pp. 1613–1630.
[15] D. Takács and G. Stépán, *Contact patch memory of tyres leading to lateral vibrations of four-wheeled vehicles*, Philosophical Transactions of the Royal Society A: Mathematical, Physical and Engineering Sciences 371 (2013).
[16] D. Takács, G. Orosz, and G. Stépán, *Delay effects in shimmy dynamics of wheels with stretched string-like tyres*, European Journal of Mechanics A/Solids 28 (2009), pp. 516–525.
[17] D. Bachrathy and G. Stépán, *Bisection method in higher dimensions and the efficiency number*, Periodica Polytechnica 56 (2012), pp. 81–86.